Retinal Angiogenesis in the Ins2^{Akita} Mouse Model of Diabetic Retinopathy

Zongchao Han,[1] *Junjing Guo,*[1] *Shannon M. Conley, and Muna I. Naash*

Purpose. Diabetic retinopathy (DR) is the leading cause of blindness among working age adults and does not have any curative treatments. Although chemical- and injury-induced models of retinal neovascularization exist, the need for a genetic model that closely simulates the DR pathologic process is great.

Methods. Here we characterize the development of the retinal disease phenotype in a genetic model of type 1 diabetes, the Ins2^{Akita} mouse, using structural, biochemical, molecular biological, and functional techniques.

Results. This model exhibits hyperglycemia by 2 months of age and by 6 months we detect retinal complications in Ins2^{Akita} males, including early signs of vascular damage consistent with DR, specifically the appearance of pericyte ghosts, vascular leakage, and microaneurysm formation. By 9 months of age, these changes are accompanied by later vascular signs of DR, specifically retinal neovascularization, formation of new capillary beds, and the presence of new blood vessels abnormally localized in the outer plexiform layer. Consistent with the debilitating effects of such vasculopathy, we also observe increased retinal apoptosis and decreased retinal function measured by electroretinogram.

Conclusions. These data indicate that the Ins2^{Akita} mouse is a good model for later-onset DR, modeling both early and some late disease signs. Furthermore, this work suggests that this model may be suitable for testing and development of targeted DR therapies. (*Invest Ophthalmol Vis Sci.* 2013;54:574–584) DOI:10.1167/iovs.12-10959

Diabetic retinopathy (DR) is a severe complication of diabetes and is the leading cause of blindness in people of working age.[1] DR is primarily a vascular disease and hyperglycemia is a critical mediator leading to vascular damage.[2] DR has two distinct phases, an early nonproliferative phase characterized by increased vascular permeability and intraretinal hemorrhages and a late proliferative phase characterized by retinal neovascularization.[3] These proliferative changes are usually accompanied by unavoidable vision loss. The mechanisms underlying DR-associated retinal damage are poorly understood, although hypoxia and accompanying upregulation of vascular endothelial growth factor (VEGF) are thought to play a part.[4] There is great need for a good model of the disease process both to further our understanding of the underlying pathophysiology and to facilitate development of effective therapeutics.

According to the US Department of Health and Human Services, 7.8% of Americans have diabetes, among whom approximately 25% possess no knowledge of having this disease or have only symptoms that are associated with complications of diabetes such as DR. Controlling blood glucose levels can prevent development of vascular complications,[5] although if diabetes is diagnosed after complications have developed the optimal time for preventive treatment has usually passed. Therefore, along with control of blood sugar, there is considerable need to explore therapeutic strategies concentrating on these vascular complications. Many clinical trials testing novel DR therapies are either ongoing or completed (e.g., NCT00604383, NCT00131144, NCT00445003, NCT00600262). As just one positive example, recently, Phase III clinical trials have been completed using ruboxistaurin (NCT00604383), a protein kinase C inhibitor, to target nonproliferative DR. Patients treated with ruboxistaurin were found to have delayed progression of DR.[6–8] Laser photocoagulation surgery, which destroys areas of the retina, has also been found to reduce/delay progression of the disease, but the procedure also destroys neural tissues. Although exciting results from these trials improve the prognosis for DR, there are still no curative therapies available, and significant room for development of additional therapies exists.

Although chemically and surgically induced models of DR/neovascularization exist, they often do not fully model the systemic diabetes/DR disease process. As a result, effort has been placed on development and study of the Ins2^{Akita} genetic model.[9–15] This autosomal dominant type 1 diabetic model carries a single base-pair substitution in the insulin 2 gene,[9] resulting in mutant insulin 2 that causes primary pancreatic beta-cell toxicity and dysfunction.[9] Heterozygous male Ins2^{Akita} mice exhibit hyperglycemia and hypoinsulinemia by 4 to 6 weeks of age without insulitis or obesity.[13] Importantly, these mice develop complications of diabetes, including neuropathy[16] and nephropathy.[14]

Although advanced, proliferative DR has not previously been studied in Ins2^{Akita} mice; various retinal pathologies characteristic of early, nonproliferative DR have been observed in this line. Ins2^{Akita} mice exhibit increased frequency of apoptotic retinal neurons, increased vascular permeability/leakage,[12] and decreased retinal blood flow.[17] These vascular changes are accompanied by vision loss as measured by change in optomotor behavior.[18] In spite of this work, the utility of the

From the Department of Cell Biology, University of Oklahoma Health Sciences Center, Oklahoma City, Oklahoma.

[1]These authors contributed equally to the work presented here and should therefore be regarded as equivalent authors.

Supported by the National Eye Institute/National Institutes of Health Grants EY10609 (MIN), EY018656 (MIN), and EY018512 (SMC), the Foundation Fighting Blindness (MIN), the Oklahoma Center for the Advancement of Science and Technology (ZH, SMC, and MIN), and the Dr. William "Bill" W. Talley II Research Award (ZH).

Submitted for publication September 13, 2012; revised November 8, 2012; accepted November 27, 2012.

Disclosure: **Z. Han**, None; **J. Guo**, None; **S.M. Conley**, None; **M.I. Naash**, None

Corresponding author: Muna I. Naash, Department of Cell Biology, University of Oklahoma Health Sciences Center, 940 Stanton L. Young Boulevard, BMSB 781 Oklahoma City, OK 73104; muna-naash@ouhsc.edu

Ins2^{Akita} line as a model for testing DR therapies is limited without characterization of late-stage disease phenotype. Here, we plot the time course of development of retinal pathology in this model and show that Ins2^{Akita} mice develop both early signs of DR (microaneurysms, vascular damage, and increased vascular leakage) and some signs of proliferative DR including neovascularization (NV) and new capillary bed formation.

Materials and Methods

Animal Husbandry

The Ins^{Akita} heterozygous male and female breeder pairs on a C57BL/6 background were kindly provided by Dr. Jason Kim at the University of Massachusetts Medical School. All mice (the Ins2^{Akita} mouse and wild-type [WT]) studied here were maintained in the breeding colony under cyclic light (12 L:12 D) conditions and received standard feed. Cages were changed twice weekly after onset of diabetes (when cages become very wet) due to diabetes-associated polyuria. All experiments and animal maintenance were approved by the University of Oklahoma Health Science Center Institutional Animal Care and Use Committee, and conformed to the *National Institute of Health Guide for the Care and Use of Laboratory Animals* and the *Association for Research in Vision and Ophthalmology Resolution on the Use of Animals in Research*. Only heterozygous male Ins2^{Akita} mice were used in experiments. Nonfasting blood glucose measurements were conducted using a glucose meter (Contour TS Blood Glucose Meter; Bayer AG, Leverkusen, Germany).

Fundus Imaging

Fundus imaging was conducted using a commercial imaging system (Micron III with mouse objective; Phoenix Research Laboratories, Pleasanton, CA). Animals were anesthetized by intramuscular injection of 85 mg/kg ketamine and 14 mg/kg xylazine (Butler Schein Animal Health, Dublin, OH). Mice were then injected intraperitoneally with 100 μL of 1% fluorescein sodium (Sigma-Aldrich, St. Louis, MO). Eyes were dilated with 1% Cyclogyl (cyclopentolate hydrochloride solution), and a drop of 2.5% methylcellulose (both from Pharmaceutical Systems, Inc., Tulsa, OK) was placed on the corneal surface. Mice were placed on an adjustable stage and the Micron III objective was stereoscopically adjusted until it came into contact with the cornea. Images were captured using a filter with excitation (486 nm) and emission (536 nm) using commercial software (StreamPix Software; Phoenix Research Laboratories).

ERG Analysis

Full-field scotopic and photopic ERG was performed on anesthetized, dilated mice after overnight dark-adaption using a visual testing system (UTAS Visual Diagnostic System; LKC Technologies, Inc., Gaithersburg, MD) as described previously.[19,20] At least 5 to 10 animals were examined per group.

Quantitative RT-PCR Analysis

qRT-PCR was performed as previously described.[21] Briefly, total RNA was extracted from the tissue of a single eye using a commercial reagent (TRIzol; Life Technologies, Inc., Carlsbad, CA) and treated with RNAse-free-DNAse I (Promega, Inc., San Luis Obispo, CA). Reverse transcription (RT) was performed using an oligo-dT primer and a reverse transcriptase (Superscript III; Life Technologies, Inc.). A no-RT (contains everything except the reverse transcriptase) sample was used as a control for residual genomic DNA. qRT-PCR was performed in triplicate on each cDNA sample using a thermal cycler (Bio-Rad C1000 Thermal Cycler; Bio-Rad, Hercules, CA) and ΔcT values for test genes were normalized to the β-actin housekeeping gene. Relative gene expression values were calculated as relative expression $= 2^{-\Delta cT}$, where ΔcT = (Gene CT − β-actin CT). Three independent qRT-PCR experiments for each set of samples were performed. We did not see any signals in the no-RT control. Agarose gel electrophoresis and disassociation curve analysis were also performed on all PCR products to confirm proper amplification. (See the Supplementary Material and Supplementary Table S1, which shows the primers used in this study, http://www.iovs.org/lookup/suppl/doi:10.1167/iovs.12-10959/-/DCSupplemental.)

Immunoblotting

Retinas were homogenized in lysis buffer (50 mM Tris [pH 7.8], 100 mM NaCl, 5 mM EDTA, 0.05% SDS, 1% TX-100, 2.5% glycerol, and 1 mM PMSF). Protein concentration was determined using the Bradford assay kit (Bio-Rad). Equal amounts of total protein were separated using 10% SDS-PAGE, and electrotransferred to PVDF membrane. Membranes were blocked with 5% nonfat milk in TBST, and incubated in anti-VEGF-A (sc-57496; Santa Cruz Biotechnology, Santa Cruz, CA), anti-VEGFR2 (sc-6251; Santa Cruz Biotechnology), or antipigment epithelium-derived growth factor (PEDF, ab14993; Abcam, Cambridge, MA) for 1 hour at room temperature. After washing, membranes were incubated with horseradish peroxidase–conjugated secondary antibodies, and visualized in accordance with the manufacturer's guidelines (Super-Signal West Dura Extended Duration Substrate; Thermo Fisher Scientific, Waltham, MA). Imaging and densitometric analysis were conducted using a commercial imaging system (Kodak Image Station 4000R; Carestream Health, Inc., Rochester, NY) and the pixel densities in each band were normalized to the amount of β-actin in each lane.

TUNEL Staining and Immunohistochemistry

Tissue fixation and sectioning were performed as previously described.[22,23] Briefly, eyes from mice at different time points were enucleated fixed and dissected with phosphate-buffered saline containing 4% paraformaldehyde at 4°C for 1 hour. Eyecups were sequentially immersed in 10%, 20%, and 30% (w/v) sucrose solutions, embedded in M1 embedding medium (Thermo Fisher Scientific), and frozen sections (10-μm thickness) were cut along the vertical meridian. The entire eye was sectioned, and every tenth section was collected. TUNEL labeling was carried out according to the manufacturer's instructions (GenScript USA, Inc., Piscataway, NJ). Briefly, tissue sections were permeabilized then incubated with terminal deoxyribonucleotidyl transferase (TdT) and biotinylated dUTP, at 37°C for 1 hour and further incubated with FITC-conjugated streptavidin for visualization. Negative controls (every procedure except TdT incubation), and positive controls (pretreatment with DNase I) were also included. The total number of TUNEL-positive cells was counted in six separate sections of each retina along the superior–inferior plane. The number of apoptotic cells/section for each eye was an average of the values for each section, $n = 3$ to 4 eyes/group. Immunohistochemistry (IHC) was performed as previously described using rat monoclonal anti-CD105 (cat. no. MAB1320) antibody (R&D Systems, Inc., Minneapolis MN). After incubation with appropriate fluorescent secondary antibody and mounting, slides were imaged using a spinning disk confocal microscope (BX62; Olympus, Tokyo, Japan) and commercial software (SlideBook version 4; Silicon Graphics, Inc., Fremont, CA). Images were taken at 435 μm (the width of a ×40 image) from the optic nerve head, and three to five animals per group/age were examined.

Hematoxylin and Eosin (H&E) Staining, Electron Microscopy, and Morphometric Analysis

Fixed eyes were dehydrated, embedded in paraffin, sectioned (10 μm), and stained with H&E using standard procedures; three to six eyes/group and age were examined. Electron microscopy (EM) on ultrathin plastic sections along the nasal/temporal plane was performed using an electron microscope (100CX; JEOL, Tokyo, Japan) as described previously.[20,24,25] Ultrastructural measurements of vascular basement

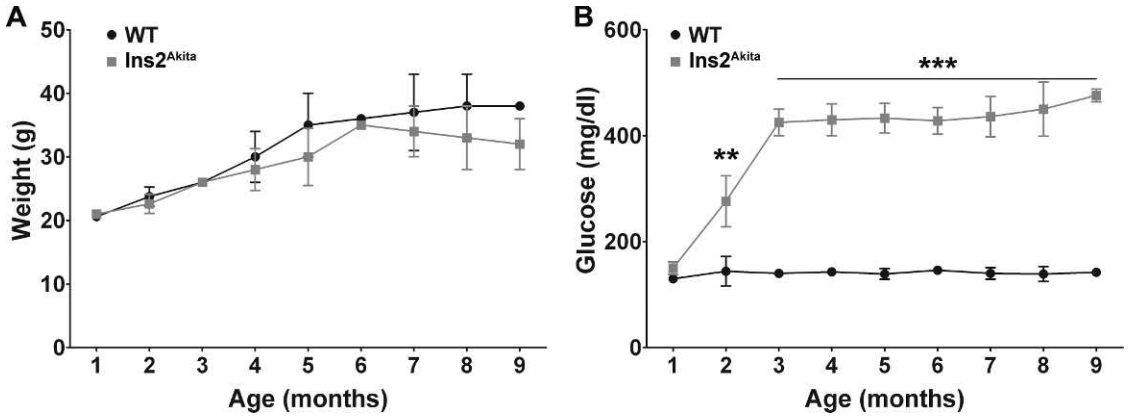

Figure 1. Ins2^{Akita} mice exhibit hyperglycemia without obesity. Nonfasting blood glucose levels and body weight of WT and Ins2^{Akita} mice were measured monthly from 1 to 9 months of age. All mice were fed a regular diet. (**A**) No significant differences in body weight were detected between WT and Ins2^{Akita} mice during the 9-month study period. (**B**) There was a significant increase in glucose levels in Ins2^{Akita} animals compared with WT, first apparent at 2 months of age. Values are mean ± SE. $^{**}P < 0.01$ and $^{***}P < 0.001$ by two-way ANOVA (age and genotype) with Bonferroni's post hoc comparisons ($n = 10$ mice/group).

membrane thickness were conducted using a photoediting device (Adobe Photoshop CS5; Adobe Systems, San Jose, CA). The basement membrane was measured at six different points around the perimeter of each vessel. These values were averaged to give a per vessel value. In all, 13 WT retinal vessels (from two mice) and 37 Ins2^{Akita} retinal vessels (from five mice) at 9 months of age were measured.

Fluorescein–Dextran Perfused Retinal Flat Mounts

One milliliter of PBS containing 50 mg/mL FITC–dextran (fluorescein isothio-cyanate-dextran; MW, 2×10^6 Daltons; Sigma-Aldrich) was injected into the left ventricle of anesthetized mice. Eyes were enucleated immediately after perfusion of FITC–dextran and fixed in 4% paraformaldehyde for 1 hour. Retinas were flat-mounted and imaged using a spinning disk confocal microscope. For quantification, ImageJ software (developed by Wayne Rasband, National Institutes of Health, Bethesda, MD; available at http://rsbweb.nih.gov/ij/index.html) was used to outline areas of vascular tuft. The total vascular area (in pixels) was expressed as a percentage of the area of the whole retina (in pixels, $n = 3$–4 eyes/group).

Statistical Analysis

Results are presented as mean ± SEM. Two-way ANOVA (genotype and age) was used to analyze differences between groups and was followed by post hoc Bonferroni's pairwise comparisons. $P < 0.05$ was regarded as statistically significant. Two-tailed Student's *t*-test was used to test the hypothesis that the basement membrane is thicker in Ins2^{Akita} mice than that in WT mice.

Results

Onset of Hyperglycemia in the Ins2^{Akita} Model

Ins2^{Akita} mice were genotyped using PCR primers specific for the mutant sequences (see the Supplementary Material and Supplementary Fig. S1, http://www.iovs.org/lookup/suppl/doi:10.1167/iovs.12-10959/-/DCSupplemental). Mice homozygous for the Ins2^{Akita} mutant allele exhibit postnatal lethality (rarely surviving beyond 12 weeks of age), and heterozygous female mice exhibit a less severe diabetic phenotype than that of males. Therefore, only heterozygous male mice were included in this study. WT littermates were used as controls. Previously, the Ins2^{Akita} mice have been shown to be viable and fertile without obesity or insulitis.[12,13] Consistent with previous results, we observed no significant difference in weight between Ins2^{Akita} mice and WT littermates (Fig. 1A). Also consistent with previous studies, we observed pronounced, persistent hyperglycemia first becoming significant at 2 months of age (Fig. 1B). To confirm that our breeder pairs were producing animals similar to those used in other studies, we also assessed glucose levels in female mice and found, in common with other groups, that the hyperglycemia in females was significantly less pronounced (not shown).

Ultrastructural Signs of Vascular Damage in the Ins2^{Akita} Model

Retinal neovascularization is a severe problem in DR, and this phenotype can occur in response to damage to existing vasculature. Vascular damage, including pericyte loss, basement membrane thickening, and microaneurysm formation, is a pathologic hallmark of DR. As a result, we assessed ultrastructural changes in retinal vasculature of Ins2^{Akita} mice. To determine whether the vascular basement membrane is thicker in Ins2^{Akita} mice than that in WT mice, basement membrane thickness was measured (Fig. 2A, white arrows) at 9 months of age. To control for variations in thickness around the vessel, measurements were taken at six different places around the circumference of each vessel and averaged. Compared with the age-matched WT, the capillary basement membrane thickness was increased by approximately 17% in Ins2^{Akita} mice (Fig. 2B, $^{*}P < 0.05$). Our results indicate that the Ins2^{Akita} mouse exhibits basement membrane defects characteristic of diabetic retinopathy observable by 9 months of age.

Angiographic Analysis of Retinal Neovascularization in the Ins2^{Akita} Model

To visualize retinal neovascularization, vascular leakage, and microaneurysms, we performed fluorescein angiography on Ins2^{Akita} mice and WT controls. Beginning at 6 months of age and worsening at 9 months of age, microaneurysm formation (Fig. 3A, red arrows) can be readily visualized and detected in Ins2^{Akita} eyes compared with age-matched WT mice. In addition, at 9 months of age, increased fluorescein leakage, indicative of increased vascular permeability, and retinal neovascularization/formation of new capillary beds are also observed. Using ImageJ software, the amount of vasculature (as a function of retinal area) was calculated and is plotted in

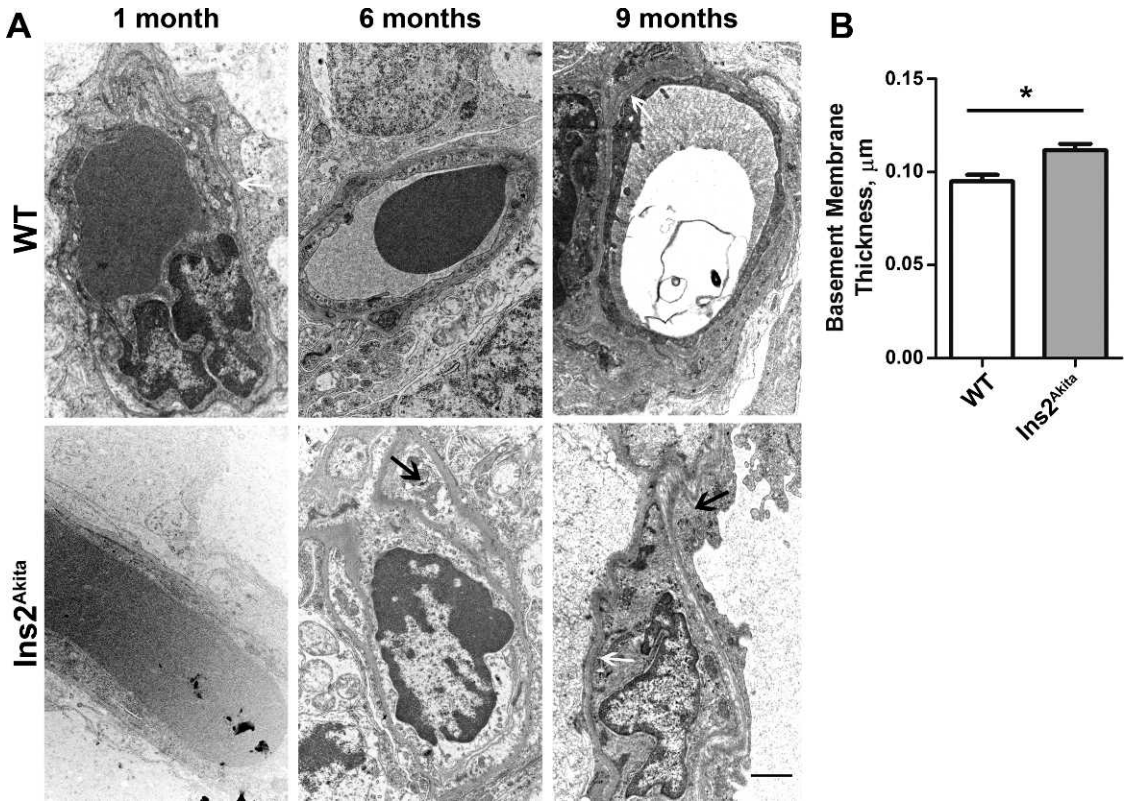

Figure 2. Ultrastructural signs of vascular pathology are detected in the Ins2^{Akita} retina. (**A**) Representative electron micrographs of retinal capillary ultrastructure from the inner nuclear layer are shown. *Black arrows* point to pericyte ghosts detectable at increased frequency in the Ins2^{Akita}. *White arrow* highlights the basement membrane. $n = 2$–5 mice/group. Scale bar, 2 μm. (**B**) Vascular basement membrane thickness was measured in 13 WT retinal vessels (from two mice) and 37 Ins2^{Akita} retinal vessels (from five mice) at 9 months of age. Basement membrane thickness was measured at six locations around the perimeter of the vessel and averaged to give a value for each vessel. $^{*}P = 0.0117$ in two-sided Student's *t*-test.

Figures 3B, 3C. We observed a significant increase in vascular area in Ins2^{Akita} mice at both 6 and 9 months of age (compared with 1 month of age). WT eyes exhibited no increase in vasculature over this time period.

To assess retinal neovascularization and vascular leakage in another way, a separate set of animals underwent intracardiac perfusion with high-molecular-weight FITC–dextran, and retinal flatmounts were subsequently imaged. FITC–dextran is retained in intact blood vessels, and this method is an efficient and valuable way to visualize and quantify retinal neovascularization and vascular leakage.[26,27] Examination of retinal flatmounts shows pronounced vascular leakage (Fig. 4A, red arrows) at 6 and 9 months of age in Ins2^{Akita} mice. In addition, we observed substantial new capillary formation in 9-month-old Ins2^{Akita} retinas (Fig. 4A, yellow arrows). There are no signs of altered vasculature in WT control animals. Using ImageJ software, the vascular area over the entire flat mount was quantified. Consistent with the results from fluorescein angiography, a statistically significant increase in vascular area was found in Ins2^{Akita} mice at 6 months of age compared with age-matched WT mice, a finding that was exacerbated in 9-month-old animals (Figs. 4B, 4C).

Structural and Immunofluorescent Signs of Vascular Pathology in the Ins2^{Akita} Model

Since we observed significant signs of neovascularization by fluorescein angiography and FITC–dextran perfusion, we examined retinal sections for signs of neoangiogenesis, particularly in retinal layers that do not normally exhibit blood vessels. Capillaries usually extend into the deep vascular plexus of the inner plexiform and inner nuclear layer (INL) after birth.[28] In contrast, in the mammalian retina the outer plexiform layer (OPL) and outer nuclear layers (ONLs) tend to be free of vessels.[28,29] No abnormal vasculature was detected on H&E-stained sections from WT animals at any age (Fig. 5A, top row), or in Ins2^{Akita} retinal sections at 1 month of age (Fig. 5A, bottom row). However, at 6 months of age Ins2^{Akita} mice began to exhibit blood vessels in the OPL (Fig. 5A, arrows), a phenotype that became more pronounced at 9 months of age.

To further confirm the identity of these abnormal vessels, frozen retinal cross-sections were labeled with antibodies against CD105 (a marker for neoangiogenesis[30]). Little or no CD105 immunoreactivity was detected in WT mice at any age and in Ins2^{Akita} mice at 1 and 6 months of age; however, significant vessel labeling was detected in both the INL and OPL at 9 months of age in Ins2^{Akita} retinas (Fig. 5B, bottom row), consistent with pronounced neovascularization at this age. Collectively, data from Figures 2 to 5 indicate that Ins2^{Akita} animals exhibit age-related vascular pathology consistent with DR, specifically retinal neovascularization, microaneurysm formation, and vascular leakage. Importantly, however, we did not observe any signs of preretinal neovascularization on histologic sections from WT or Ins2^{Akita} mice, suggesting that this common phenotype of proliferative DR is not modeled by the Ins2^{Akita} mouse, although we cannot rule out the possibility that it will appear at later time points.

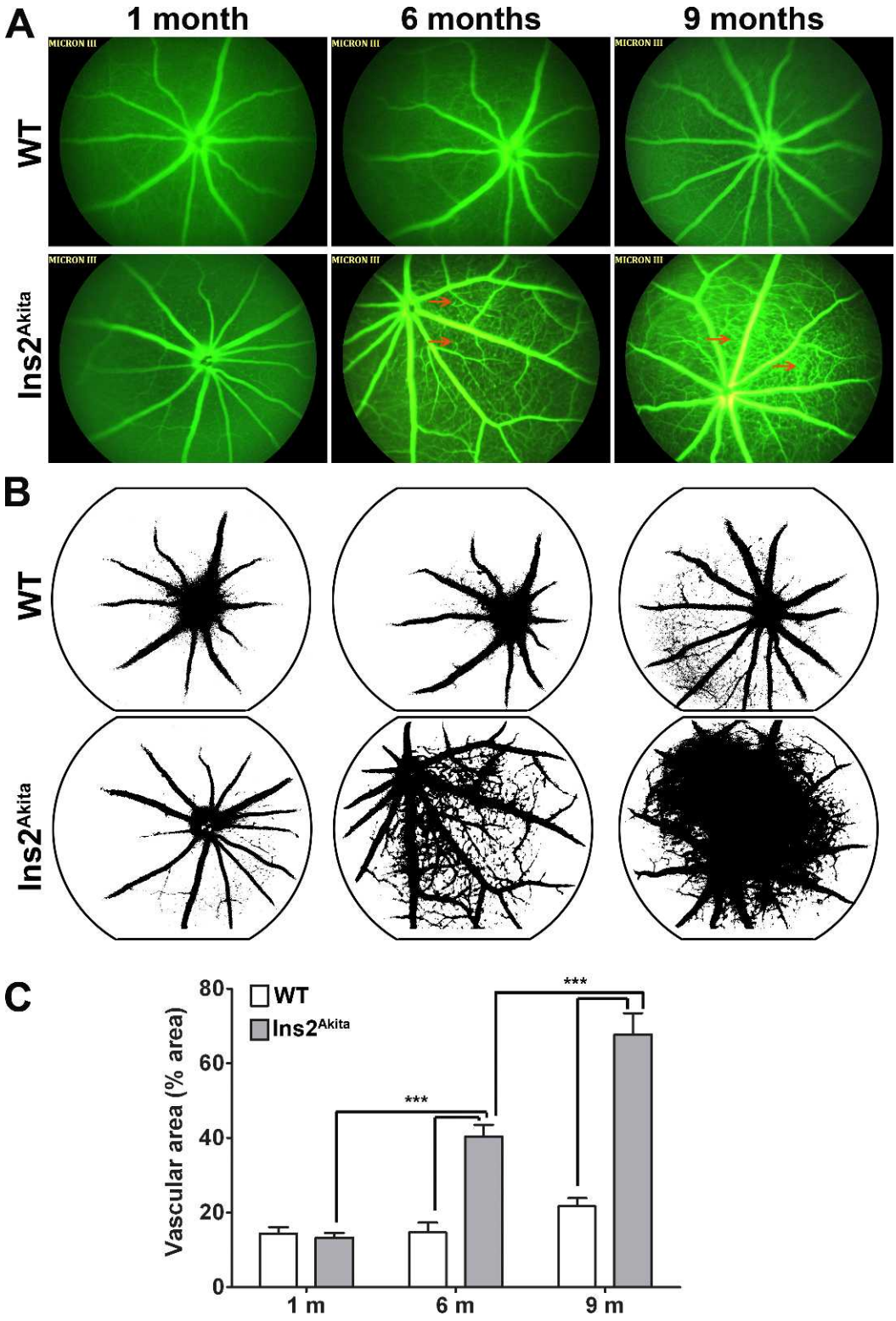

Figure 3. Fluorescein angiography shows retinal neovascularization in Ins2^{Akita} animals. (**A**) Fluorescein angiography photographs from WT and Ins2^{Akita} mice were taken at 1, 6, and 9 months of age. Early signs of neovascularization (new vessel arcade) and microaneurysms (*red arrows*) are observed in 6-month-old Ins2^{Akita} mice. More progressive neovascularization is apparent in Ins2^{Akita} eyes at 9 months of age. (**B**, **C**) NIH ImageJ was used to evaluate the vascular area (occupied by green fluorescence) in each eye. Values are mean ± SE. $^{***}P < 0.001$ by two-way ANOVA (age and genotype) with Bonferroni's post hoc comparisons ($n = 4$ mice/group).

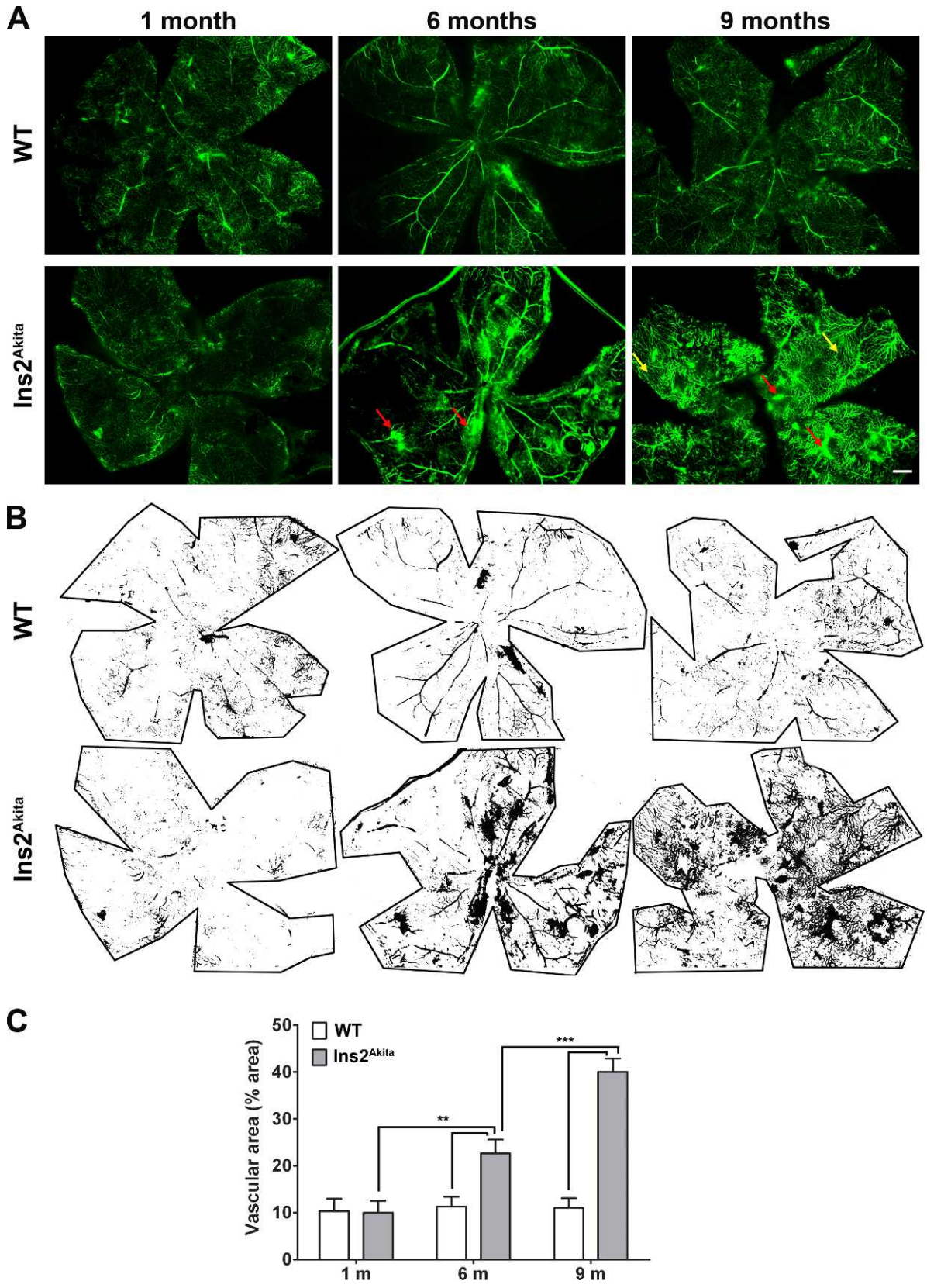

Figure 4. Fluorescein–dextran perfused retinal flat mounts from Ins2^{Akita} mice show vascular leakage and new capillary bed formation. (**A**) Animals underwent cardiac perfusion with high molecular weight fluorescein–dextran. Retinal flatmounts were imaged using a confocal microscope. The retinal vascular network was easily visible in all eyes. Retinal neovascularization and vascular leakage (*red arrows*) was detected in Ins2^{Akita} flatmounts at 6 and 9 months of age. Significant new capillary bed formation is also detected in Ins2^{Akita} retinas (*yellow arrows*). Scale bar, 500 μm. (**B**, **C**) Whole-mount retinas stained with FITC-dextran were analyzed using ImageJ software as in Figure 5. Values are mean ± SE. $^{**}P < 0.01$, $^{***}P < 0.001$ by two-way ANOVA (age and genotype) with Bonferroni's post hoc comparisons ($n = 4$ eyes/group).

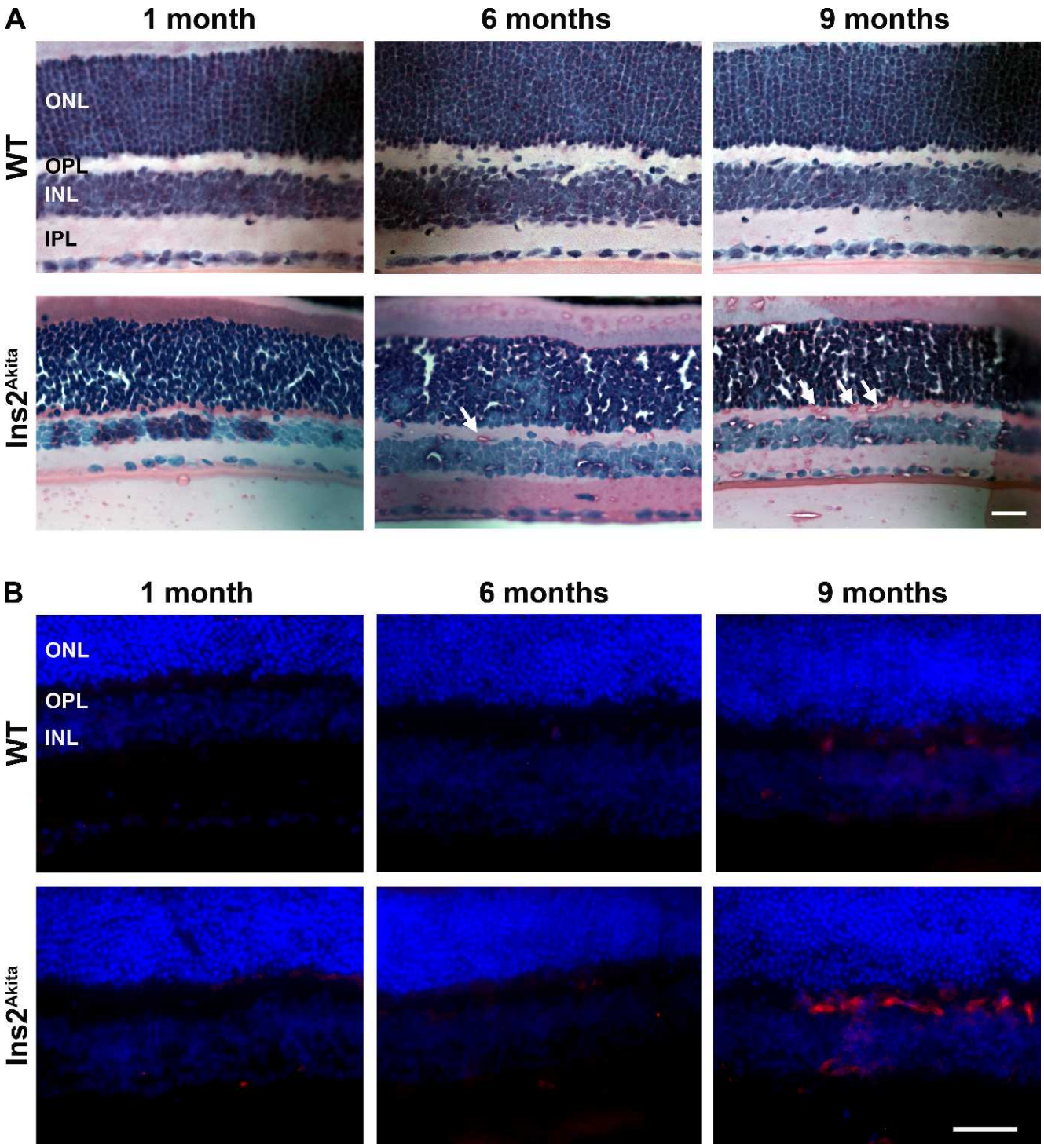

Figure 5. Histologic evidence of retinal neovascularization is seen in the $Ins2^{Akita}$ mice. (**A**) H&E-stained retinal sections from $Ins2^{Akita}$ (*bottom row*) and WT control (*top row*) mice were examined at 1, 6, and 9 months of age. *White arrows* indicate new blood vessels formed in the OPL of $Ins2^{Akita}$ mice. No such vessels are observed in WT controls at any age. Scale bar, 25 μm. (**B**) Frozen retinal sections were labeled with antibodies against CD105 (*red*), a marker for neoangiogenesis, and counterstained with DAPI (*blue*). Red labeling indicates there is substantial neovascularization in $Ins2^{Akita}$ retinas at 9 months of age, whereas no labeling is detected in WT retinas. Scale bar, 40 μm. $n = 3$–4 eyes/group.

Imbalance in Pro- and Antiangiogenic Factors in $Ins2^{Akita}$ Eyes

Angiogenic growth factors, such as VEGF-A and VEGFR2, are critical for new blood vessel growth.[31,32] Neovascularization during DR can be caused by imbalance between these angiogenic factors and antiangiogenic factors such as PEDF.[33–35] To determine whether the balance between pro- and antiangiogenic factors is altered in $Ins2^{Akita}$ retinas, VEGF-A, VEGFR2, and PEDF mRNA and protein levels were assessed (Figs. 6A–C). VEGF-A and VEGFR2 mRNA and protein levels were significantly elevated in $Ins2^{Akita}$ eyes at 9 months of age.

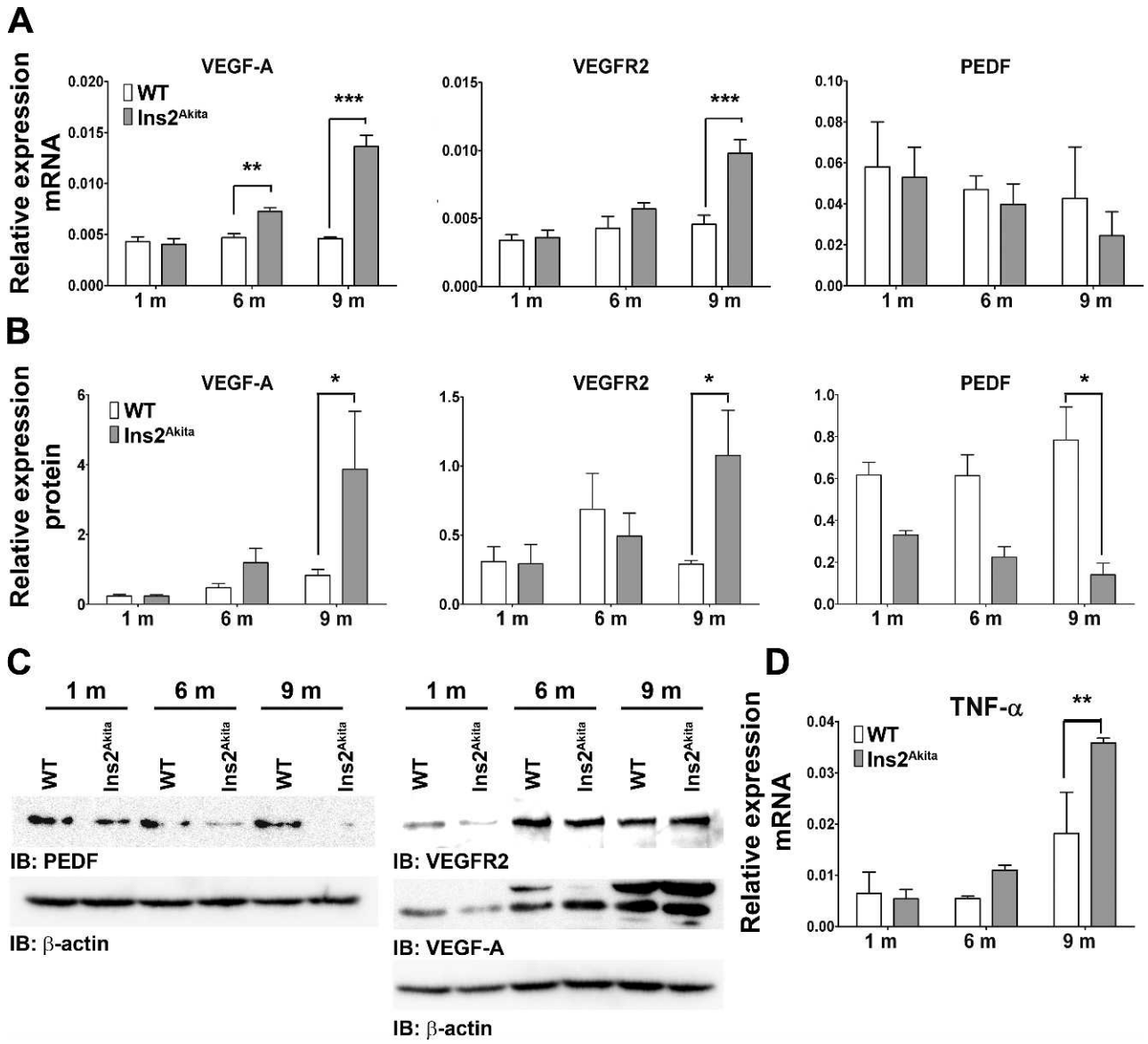

Figure 6. Ins2^{Akita} eyes exhibit an imbalance in pro- and antiangiogenic factors. Key DR-related proangiogenic factors, VEGF-A and VEGFR2, and the antiangiogenic factor PEDF were evaluated in Ins2^{Akita} and WT eyes on the message (qRT-PCR, **A**) and protein (SDS-PAGE/Western blot, **B–C**) level. Message and protein levels were normalized to β-actin. (**C**) Representative Western blots of retinas isolated from WT and Ins2^{Akita} animals. Band size for VEGFR2 is 150 kDa, for VEGF-A is 43 kDa, and for PEDF is 50 kDa. (**D**) TNF-α message levels were assessed by qRT-PCR for all groups and normalized to β-actin. All values are mean ± SE. $^{*}P < 0.05$, $^{**}P < 0.01$, and $^{***}P < 0.001$ by two-way ANOVA (age and genotype) with Bonferroni's post hoc comparisons ($n = 3$ eyes/group).

In contrast, at 9 months of age, the expression of PEDF protein was significantly decreased (Figs. 6B, 6C). In addition to examining pro- and antiangiogenic factors, we also tested cytokine levels because DR-associated retinal neovascularization has previously been associated with an inflammatory response.[36,37] Consistent with this, we observed that at 9 months of age TNF-α message levels were significantly higher in Ins2^{Akita} mice than those in WT mice (Fig. 6D). These data provide biochemical support for our structural observations of vascular abnormalities in the Ins2^{Akita} eyes.

Retinal Degeneration in the Ins2^{Akita} Model

Although no gross alterations in retinal thickness were apparent in our histologic assessments (see Fig. 5), we wanted to examine whether there were any structural or functional abnormalities occurring concomitantly with the vascular defects. To look for increased apoptosis, retinal sections were TUNEL labeled, and consistent with what has been previously shown,[12] we observed a significant increase in TUNEL-positive apoptotic cells in the Ins2^{Akita} retinas at 6 and 9 months of age compared with WT retinas (see the Supplementary Material and Supplementary Fig. S2, http://www.iovs.org/lookup/suppl/doi:10.1167/iovs.12-10959/-/DCSupplemental).

Finally, we conducted full-field ERG on Ins2^{Akita} mice and age-matched WT controls. Although WT mice exhibited no significant reduction in either scotopic or photopic ERG amplitudes over the course of the study, Ins2^{Akita} mice exhibited significant reductions in ERG function by 9 months of age (Fig. 7). The functional deficit is most pronounced in the scotopic b-wave, in keeping with a primary effect on second-order neurons rather than photoreceptors. These data indicate

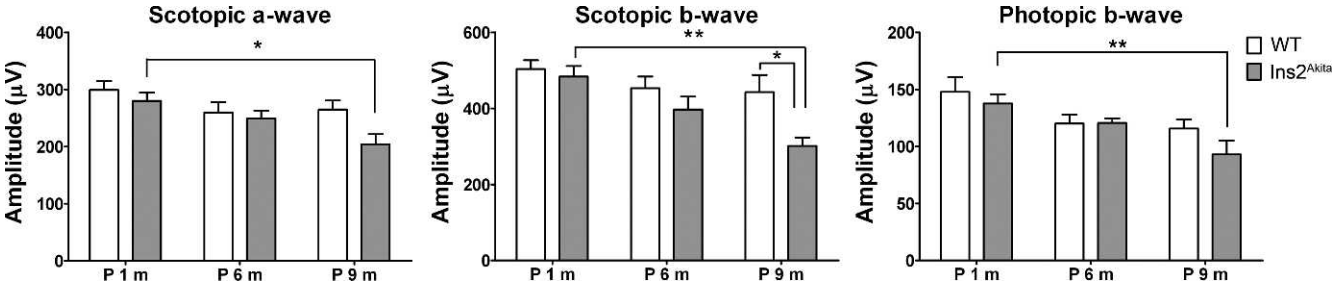

Figure 7. Aged Ins2^{Akita} animals exhibit decreased retinal function. Full-field scotopic and photopic ERG were conducted on Ins2^{Akita} animals and age-matched WT controls at 1, 6, and 9 months of age. Scotopic a-wave, b-wave, and photopic b-wave amplitudes decreased significantly at 9 months of age in Ins2^{Akita} mice compared with Ins2^{Akita} mice at 1 month of age. A significant reduction in scotopic b-wave between WT and Ins2^{Akita} mice was also detected at 9 months of age. Values are mean ± SE. $^{*}P < 0.05$ and $^{**}P < 0.01$ by two-way ANOVA (age and genotype) with Bonferroni's post hoc comparisons ($n = 10$ mice/group).

that visual function is adversely affected in the aged Ins2^{Akita} mouse, consistent with the previously described debilitating effects of retinal neovascularization.[38,39] These data further show that the Ins2^{Akita} mouse models both DR-associated vascular complications and DR-associated vision loss.

Discussion

The Ins2^{Akita} mice have been previously shown to exhibit many early signs of DR: specifically, retinal neuronal loss, development of early stage vascular damage (such as pericyte loss, an increased number of acellular capillaries, and increased vascular permeability), and vision loss as measured by alterations in optomotor behavior (contrast sensitivity and spatial frequency threshold).[10–12,18] Our data support these prior observations. We here report increased vascular leakage, retinal apoptosis, modest thickening of the vascular basement membrane, and decreased retinal function as measured by ERG. However, importantly, we observed retinal neovascularization and the formation of new capillary beds. We observed this neovascularization in fundus angiograms, in dextran-perfused retinal flatmounts, in histologic sections, and by labeling with the neovascular marker CD105. It is not clear why these phenotypes have not been reported before, although they are relatively late in onset with significant neovascularization not detectable until 9 months of age. Most previous studies have not looked at animals past the age of 6 months, an age at which we see primarily signs of vascular damage, without transition to a more proliferative angiogenic disease form. It is logical that this transition from early- to late-stage disease would occur in the Ins2^{Akita} mouse. Studies have shown that basement membrane thickening and loss of pericyte coverage make retinal vessels less stable and more susceptible to T-lymphocyte–mediated apoptosis.[29] The loss of these regulatory cells disrupts the tight junctions of the blood–retinal barrier and leads to abnormal neovascularization.[40,41] In spite of the myriad signs of vascular disease we see in the Ins2^{Akita} mice, it is important to recognize that we do not detect signs of preretinal neovascularization (a common phenotype of proliferative DR), in these mice, and studies targeting this particular phenotype may need to consider other models such as the opticin knockout mouse[42] or the oxygen-induced retinopathy model.[43,44]

The retinal microangiopathy caused by diabetes is a complex disease that is strictly controlled by a spectrum of pro- and anti-inflammatory factors, pro- and antiangiogenic factors, as well as other factors such as proteases, extracellular matrix proteins, chemokines, vasoactive hormones, immune cells, and adhesion molecules.[45–47] Changes in other pathways such as the oxidative stress pathway,[48] the nonspecific inflammation pathway,[49] and the endoplasmic reticulum stress pathway[50] have also been reported in DR. Together, these changes constitute a complex aberrant network in DR. Clearly, there is no single factor or single pathway involved in or triggered by DR. The Ins2^{Akita} mouse does exhibit changes in some of these pathways. For example, it has been shown that these mice exhibit signs of oxidative stress, including accumulation of oxidized and glycated lipids and reactive nitrogen species, a process thought to contribute to pericyte loss and retinal degeneration.[15,51] We show here that the Ins2^{Akita} mice exhibit increased levels of the inflammatory marker TNF-α, and others have also reported increases in inflammatory mediators in the Ins2^{Akita} model,[52] suggesting that alterations in this pathway are also modeled by the Ins2^{Akita} mouse. Similarly, work has shown that ER stress markers such as GRP78 and phosphor-IRE1a are upregulated in the Ins2^{Akita} mouse.[50] Further elucidation of the complex underlying DR pathobiology and the role played by these various pathways will contribute to the optimal therapeutic development.

There is a significant need for a genetic model for chronic DR to facilitate development of treatments and further our understanding of the DR disease process. Although chemical or injury-induced models of neovascularization can provide useful information, they often do not accurately model the chronic, systemic nature of the diabetic/DR disease process, and side effects of chemicals cannot be overlooked. The data we show here indicating that the Type 1 diabetic Ins2^{Akita} mouse exhibits signs of both early and late DR suggest that this mouse model may be suitable for testing and developing therapies designed to target DR.

Acknowledgments

The authors thank Barb Nagel and Rasha S. Makkia for technical assistance, and Jian-Xing Ma for critical discussions on this study.

References

1. Antonetti DA, Barber AJ, Bronson SK, et al. Diabetic retinopathy: seeing beyond glucose-induced microvascular disease. *Diabetes*. 2006;55:2401–2411.
2. Ruderman NB, Williamson JR, Brownlee M. Glucose and diabetic vascular disease. *FASEB J*. 1992;6:2905–2914.
3. Calcutt NA, Cooper ME, Kern TS, Schmidt AM. Therapies for hyperglycaemia-induced diabetic complications: from animal models to clinical trials. *Nat Rev Drug Discov*. 2009;8:417–429.
4. Pe'er J, Folberg R, Itin A, Gnessin H, Hemo I, Keshet E. Upregulated expression of vascular endothelial growth factor

in proliferative diabetic retinopathy. *Br J Ophthalmol*. 1996; 80:241–245.

5. Teixeira AS, Andrade SP. Glucose-induced inhibition of angiogenesis in the rat sponge granuloma is prevented by aminoguanidine. *Life Sci*. 1999;64:655–662.
6. Sahu AK, Majji AB. Effect of ruboxistaurin on the visual acuity decline associated with long-standing diabetic macular edema. *Invest Ophthalmol Vis Sci*. 2010;51:6890; author reply 6890–6891.
7. Aiello LP, Vignati L, Sheetz MJ, et al. Oral protein kinase C beta inhibition using ruboxistaurin: efficacy, safety, and causes of vision loss among 813 patients (1,392 eyes) with diabetic retinopathy in the Protein Kinase C beta Inhibitor-Diabetic Retinopathy Study and the Protein Kinase C beta Inhibitor-Diabetic Retinopathy Study 2. *Retina*. 2011;31:2084–2094.
8. Sheetz MJ, Aiello LP, Shahri N, Davis MD, Kles KA, Danis RP. Effect of ruboxistaurin (RBX) on visual acuity decline over a 6-year period with cessation and reinstitution of therapy: results of an open-label extension of the Protein Kinase C Diabetic Retinopathy Study 2 (PKC-DRS2). *Retina*. 2011;31:1053–1059.
9. Wang J, Takeuchi T, Tanaka S, et al. A mutation in the insulin 2 gene induces diabetes with severe pancreatic beta-cell dysfunction in the Mody mouse. *J Clin Invest*. 1999;103:27–37.
10. Gastinger MJ, Kunselman AR, Conboy EE, Bronson SK, Barber AJ. Dendrite remodeling and other abnormalities in the retinal ganglion cells of Ins2^{Akita} diabetic mice. *Invest Ophthalmol Vis Sci*. 2008;49:2635–2642.
11. Gastinger MJ, Singh RS, Barber AJ. Loss of cholinergic and dopaminergic amacrine cells in streptozotocin-diabetic rat and Ins2^{Akita}-diabetic mouse retinas. *Invest Ophthalmol Vis Sci*. 2006;47:3143–3150.
12. Barber AJ, Antonetti DA, Kern TS, et al. The Ins2^{Akita} mouse as a model of early retinal complications in diabetes. *Invest Ophthalmol Vis Sci*. 2005;46:2210–2218.
13. Yoshioka M, Kayo T, Ikeda T, Koizumi A. A novel locus, Mody4, distal to D7Mit189 on chromosome 7 determines early-onset NIDDM in nonobese C57BL/6 (Akita) mutant mice. *Diabetes*. 1997;46:887–894.
14. Gurley SB, Clare SE, Snow KP, Hu A, Meyer TW, Coffman TM. Impact of genetic background on nephropathy in diabetic mice. *Am J Physiol Renal Physiol*. 2006;290:F214–F222.
15. Smith SB, Duplantier J, Dun Y, et al. In vivo protection against retinal neurodegeneration by sigma receptor 1 ligand (+)-pentazocine. *Invest Ophthalmol Vis Sci*. 2008;49:4154–4161.
16. Schmidt RE, Green KG, Snipes LL, Feng D. Neuritic dystrophy and neuronopathy in Akita (Ins2(Akita)) diabetic mouse sympathetic ganglia. *Exp Neurol*. 2009;216:207–218.
17. Wright WS, Yadav AS, McElhatten RM, Harris NR. Retinal blood flow abnormalities following six months of hyperglycemia in the Ins2(Akita) mouse. *Exp Eye Res*. 2012;98:9–15.
18. Akimov NP, Renteria RC. Spatial frequency threshold and contrast sensitivity of an optomotor behavior are impaired in the Ins2^{Akita} mouse model of diabetes. *Behav Brain Res*. 2012; 226:601–605.
19. Chakraborty D, Conley SM, Stuck MW, Naash MI. Differences in RDS trafficking, assembly, and function in cones versus rods: insights from studies of C150S-RDS. *Hum Mol Genet*. 2010;19:4799–4812.
20. Ding XQ, Nour M, Ritter LM, Goldberg AF, Fliesler SJ, Naash MI. The R172W mutation in peripherin/rds causes a cone-rod dystrophy in transgenic mice. *Hum Mol Genet*. 2004;13:2075–2087.
21. Han Z, Koirala A, Makkia R, Cooper MJ, Naash MI. Direct gene transfer with compacted DNA nanoparticles in retinal pigment epithelial cells: expression, repeat delivery and lack of toxicity. *Nanomedicine (Lond)*. 2012;7:521–539.
22. Farjo R, Skaggs J, Quiambao AB, Cooper MJ, Naash MI. Efficient non-viral ocular gene transfer with compacted DNA nanoparticles. *PLoS ONE*. 2006;1:e38.
23. Cai X, Conley SM, Nash Z, Fliesler SJ, Cooper MJ, Naash MI. Gene delivery to mitotic and postmitotic photoreceptors via compacted DNA nanoparticles results in improved phenotype in a mouse model of retinitis pigmentosa. *FASEB J*. 2010;24: 1178–1191.
24. Tan E, Wang Q, Quiambao AB, et al. The relationship between opsin overexpression and photoreceptor degeneration. *Invest Ophthalmol Vis Sci*. 2001;42:589–600.
25. Han Z, Conley SM, Makkia RS, Cooper MJ, Naash MI. DNA nanoparticle-mediated ABCA4 delivery rescues Stargardt dystrophy in mice. *J Clin Invest*. 2012;122:3221–3226.
26. Lai CC, Wu WC, Chuang LH, Yeung L, Wei W, Yang KJ. Quantitative grading of preretinal neovascularization in adult rats. *Acta Ophthalmol Scand*. 2005;83:590–594.
27. Edelman JL, Castro MR. Quantitative image analysis of laser-induced choroidal neovascularization in rat. *Exp Eye Res*. 2000;71:523–533.
28. Stone J, Dreher Z. Relationship between astrocytes, ganglion cells and vasculature of the retina. *J Comp Neurol*. 1987;255: 35–49.
29. Dorrell MI, Friedlander M. Mechanisms of endothelial cell guidance and vascular patterning in the developing mouse retina. *Prog Retin Eye Res*. 2006;25:277–295.
30. Duff SE, Li C, Garland JM, Kumar S. CD105 is important for angiogenesis: evidence and potential applications. *FASEB J*. 2003;17:984–992.
31. Relf M, LeJeune S, Scott PA, et al. Expression of the angiogenic factors vascular endothelial cell growth factor, acidic and basic fibroblast growth factor, tumor growth factor beta-1, platelet-derived endothelial cell growth factor, placenta growth factor, and pleiotrophin in human primary breast cancer and its relation to angiogenesis. *Cancer Res*. 1997;57: 963–969.
32. Folkman J, Klagsbrun M. Angiogenic factors. *Science (New York, NY)*. 1987;235:442–447.
33. Zhang SX, Wang JJ, Gao G, Parke K, Ma JX. Pigment epithelium-derived factor downregulates vascular endothelial growth factor (VEGF) expression and inhibits VEGF-VEGF receptor 2 binding in diabetic retinopathy. *J Mol Endocrinol*. 2006;37:1–12.
34. Nam DH, Oh J, Roh JH, Huh K. Different expression of vascular endothelial growth factor and pigment epithelium-derived factor between diabetic and non-diabetic epiretinal membranes. *Ophthalmologica*. 2009;223:188–191.
35. Wang JJ, Zhang SX, Lu K, et al. Decreased expression of pigment epithelium-derived factor is involved in the pathogenesis of diabetic nephropathy. *Diabetes*. 2005;54:243–250.
36. Nehme A, Edelman J. Dexamethasone inhibits high glucose-, TNF-alpha-, and IL-1beta-induced secretion of inflammatory and angiogenic mediators from retinal microvascular pericytes. *Invest Ophthalmol Vis Sci*. 2008;49:2030–2038.
37. Naldini A, Carraro F. Role of inflammatory mediators in angiogenesis. *Curr Drug Targets Inflamm Allergy*. 2005;4:3–8.
38. Neroev VV, Zueva MV, Tsapenko IV, Riabina MV, Hun L. Functional diagnostics of retinal ischemia: Muller cells and neovascularization of the retina in diabetic retinopathy [in Russian]. *Vestn Oftalmol*. 2005;121:22–24.
39. Zakareia FA, Alderees AA, Al Regaiy KA, Alrouq FA. Correlation of electroretinography b-wave absolute latency, plasma levels of human basic fibroblast growth factor, vascular endothelial growth factor, soluble fatty acid synthase, and adrenomedullin in diabetic retinopathy. *J Diabetes Complications*. 2010;24: 179–185.

40. Runkle EA, Antonetti DA. The blood-retinal barrier: structure and functional significance. *Methods Mol Biol*. 2011;686:133–148.
41. Frey T, Antonetti DA. Alterations to the blood-retinal barrier in diabetes: cytokines and reactive oxygen species. *Antioxid Redox Signal*. 2011;15:1271–1284.
42. Goff MM, Lu H, Ugarte M, et al. The vitreous glycoprotein opticin inhibits preretinal neovascularization. *Invest Ophthalmol Vis Sci*. 2012;53:228–234.
43. Taylor AC, Mendel TA, Mason KE, Degen KE, Yates PA, Peirce SM. Attenuation of ephrinB2 reverse signaling decreases vascularized area and preretinal vascular tuft formation in the murine model of oxygen-induced retinopathy. *Invest Ophthalmol Vis Sci*. 2012;53:5462–5470.
44. Xu H, Liu J, Xiong S, Le YZ, Xia X. Suppression of retinal neovascularization by lentivirus-mediated netrin-1 small hairpin RNA. *Ophthalmic Res*. 2012;47:163–169.
45. Distler JH, Hirth A, Kurowska-Stolarska M, Gay RE, Gay S, Distler O. Angiogenic and angiostatic factors in the molecular control of angiogenesis. *Q J Nucl Med*. 2003;47:149–161.
46. Gariano RF, Gardner TW. Retinal angiogenesis in development and disease. *Nature*. 2005;438:960–966.
47. Aiello LP. Angiogenic pathways in diabetic retinopathy. *N Engl J Med*. 2005;353:839–841.
48. Madsen-Bouterse SA, Kowluru RA. Oxidative stress and diabetic retinopathy: pathophysiological mechanisms and treatment perspectives. *Rev Endocr Metab Disord*. 2008;9:315–327.
49. Zhang W, Liu H, Al-Shabrawey M, Caldwell RW, Caldwell RB. Inflammation and diabetic retinal microvascular complications. *J Cardiovasc Dis Res*. 2011;2:96–103.
50. Li J, Wang JJ, Yu Q, Wang M, Zhang SX. Endoplasmic reticulum stress is implicated in retinal inflammation and diabetic retinopathy. *FEBS Lett*. 2009;583:1521–1527.
51. Zou MH, Li H, He C, Lin M, Lyons TJ, Xie Z. Tyrosine nitration of prostacyclin synthase is associated with enhanced retinal cell apoptosis in diabetes. *Am J Pathol*. 2011;179:2835–2844.
52. Freeman WM, Bixler GV, Brucklacher RM, et al. Transcriptomic comparison of the retina in two mouse models of diabetes. *J Ocul Biol Dis Inform*. 2009;2:202–213.